# Gas-Phase $Br_2$ Production in Heterogeneous Reactions of $Cl_2$, HOCl, and BrCl with Halide−Ice Surfaces

**Amy K. Huff and Jonathan P. D. Abbatt*,†**

*Department of the Geophysical Sciences, The University of Chicago, 5734 South Ellis Avenue, Chicago, Illinois 60637*

*Received: March 28, 2000; In Final Form: May 24, 2000*

In order to evaluate the relative importance of different heterogeneous mechanisms that may release gas-phase $Br_2$ into the Arctic boundary layer, interactions of $Cl_2$, HOCl, and BrCl with halide-containing ice surfaces were studied in the laboratory. Results are presented from experiments using a coated-wall, low-pressure flow tube coupled to a mass spectrometer. Gas-surface reaction probabilities were calculated from the first-order loss of $Cl_2$, HOCl, or BrCl on bromide-ice surfaces at 233 K and on chloride/bromide-ice surfaces at 248 K. In all cases, the reactions were relatively fast, and the primary product was gas-phase $Br_2$. To determine the main factors that influence the kinetics of these reactions, experiments were conducted over a range of temperatures, hydrogen ion concentrations in ice, and halide concentrations in ice. $Cl_2$ reaction probability increases with increasing bromide concentration in the ice film, up to approximately 3% bromide. At this point, the ice surface is completely saturated with bromide ions, and the maximum reaction probability is 0.1. In contrast, HOCl reaction probability is highest when the ice film is made from a solution with low pH. BrCl reaction probability on bromide-ice films is less than that of $Cl_2$ and less than or equal to that of HOCl, depending on hydrogen ion concentration. No reaction between $Cl_2$ or HOCl and chloride-ice films was observed. The impact of $Cl_2$, HOCl, and BrCl heterogeneous chemistry on catalytic ozone destruction in the Arctic boundary layer is discussed.

## Introduction

Over the past decade, ozone ($O_3$) loss in the springtime Arctic boundary layer has become a well-established phenomenon. After polar sunrise, $O_3$ mixing ratios can fall from tens of parts per billion to less than one part per billion in hours to days.[1] Low $O_3$ mixing ratios are correlated with high filterable bromine concentrations, suggesting that large amounts of active bromine compounds are present in the troposphere during periods of $O_3$ destruction.[1−3] In air masses where $O_3$ loss occurs, long path length absorption spectroscopy spectra show that elevated bromine monoxide (BrO) concentrations are widespread,[4] and $C_2$−$C_6$ hydrocarbon mixing ratio measurements indicate the presence of bromine atom (Br) chemistry.[5] Consequently, researchers have suggested that catalytic cycles involving Brand BrO are responsible for the observed $O_3$ loss.[6−12]

To destroy $O_3$ on such a short time scale, it is necessary to maintain high levels of active bromine in the atmosphere. Br and BrO rapidly convert to inactive compounds, such as HBr, HOBr and $BrNO_3$, which terminate $O_3$ loss. However, inactive bromine may recycle back into $Br_2$ on the surface of sulfate aerosol,[7,8] which could keep tropospheric concentrations of Br and BrO elevated. Modeling studies also suggest that autocatalytic mechanisms may be a means of quickly introducing large amounts of active bromine into the troposphere.[9−12] In particular, autocatalytic release of $Br_2$ may occur via HOBr uptake on acidified sea salt aerosol:[12]

Condensed-phase surface reactions:

$$HOBr + Cl^- + H^+ \rightarrow BrCl + H_2O \qquad (R1)$$

$$BrCl + Br^- \rightarrow Br_2 + Cl^- \qquad (R2)$$

Gas-phase atmospheric reactions:

$$Br_2 + h\nu \rightarrow 2Br \qquad (R3)$$

$$2[Br + O_3 \rightarrow BrO + O_2] \qquad (R4)$$

$$2[BrO + HO_2 \rightarrow HOBr + O_2] \qquad (R5)$$

$$\text{Net:} \quad Br^- + 2O_3 + 2HO_2 + H^+ \rightarrow H_2O + HOBr + 4O_2$$

This mechanism is autocatalytic because reaction of one HOBr molecule ultimately produces two new HOBr molecules, each of which can begin the cycle again. Once it is initiated, this mechanism has the potential to oxidize large amounts of bromide in a matter of days. Modeling studies have suggested that this chemistry may also operate in the marine boundary layer at lower latitudes,[10,12] where significant amounts of $O_3$ that have traveled from continental sources may be destroyed.[10]

It is not clear what chemical reactions produce the photochemically active bromine compounds that initiate catalytic $O_3$ destruction in the troposphere. There are many possibilities, including gas-phase photolysis of bromoform[1] and nitryl bromide,[13] as well as oxidation of bromide on sea salt aerosols by peroxymonosulfuric acid.[9] Alternatively, McConnell et al.[6] and Tang and McConnell[11] have suggested that active bromine may arise from heterogeneous interactions between the atmosphere and sea salt components in surface snow. Central to their theory is the idea that concentrated sea salt bromide, deposited by aerosols or sea spray, may be converted into $Br_2$ in the coastal snowpack. After degassing into the atmosphere, $Br_2$ photolyzes to produce bromine radicals that can initiate $O_3$ destruction.

We present here experimental kinetic studies of the interactions of gas-phase chlorine ($Cl_2$), hypochlorous acid (HOCl), and bromine chloride (BrCl) with halide-ice surfaces. There is

---

* Corresponding author.

† Current address: Department of Chemistry, University of Toronto, 80 St. George Street, Toronto, Ontario M5S 3H6 Canada. E-mail: jabbatt@alchemy.chem.utoronto.ca.

10.1021/jp001155w CCC: $19.00

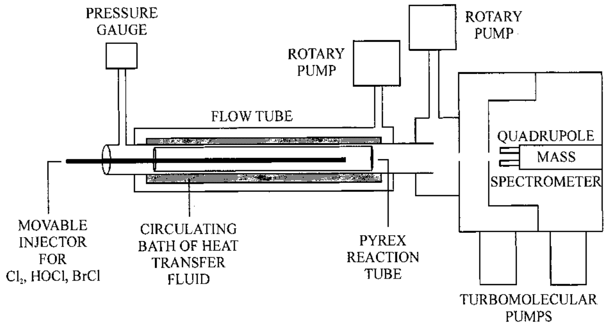

**Figure 1.** Schematic diagram of the low-pressure flow tube-mass spectrometer system.

increasing evidence from field measurements that $Cl_2$ and HOCl may contribute significantly to the oxidation capacity of the lower troposphere,[14,15] particularly during $O_3$ loss events. As a result, we begin by studying the heterogeneous reactions of these gases. Although there is some question as to whether the initial steps in the $O_3$ destruction chemistry occur on aerosols or surfaces, we follow the suggestion of McConnell et al.[6] and Tang and McConnell[11] and focus on simulated sea ice surfaces. In conjunction with field measurements of active chlorine compounds,[14] our experimental data indicate that gas-phase $Br_2$ formed from interactions of $Cl_2$ and HOCl with sea ice may be sufficient to initiate ozone destruction in the Arctic troposphere. This study demonstrates that these heterogeneous reactions need to be considered alongside other mechanisms that have been proposed to explain bromide oxidation in the boundary layer.

To evaluate the parameters that influence the kinetics of these reactions, experiments were conducted at two different temperatures and over a range of hydrogen ion, bromide, and chloride concentrations in ice. We began by studying simple halide-ice surfaces and gradually increased their complexity until they resembled natural sea ice. This work is the first investigation of gas-phase $Br_2$ formation from $Cl_2$ or HOCl interactions with simulated sea ice surfaces at temperatures representative of the springtime Arctic boundary layer. However, active bromine compounds have been observed as the products of many analogous reactions. In particular, $Cl_2$ reacts with solid NaBr[16] and solid sea salts[17] to produce gas-phase $Br_2$ and BrCl; $Cl_2$ also reacts with HBr on ice[18] to form $Br_2$. HOCl reacts readily with HBr on ice[19] to produce BrCl and $Br_2$ and on cold sulfuric acid surfaces[8] to make BrCl. Both BrCl and $Br_2$ are also observed as products in reactions of HOBr with sea salt doped ice surfaces[20] and aqueous salt solutions.[21] In addition, $O_3$ reacts with seawater ice[22] to produce $Br_2$ and with sodium halide particles[23] and a nitric acid/salt solution[24] to form BrCl and $Br_2$.

## Experimental Section

Experiments were conducted in a horizontal low-pressure flow tube coupled to an electron-impact quadrupole mass spectrometer. A schematic diagram of the experimental system is shown in Figure 1. Halide-ice films were made by coating the inner wall of a 2.34 cm i.d. Pyrex reaction tube with approximately 1 mL of aqueous NaBr, NaCl, or NaCl/NaBr solution. NaBr and NaCl solutions were made by dissolving known amounts of NaBr salt (Fisher Scientific) or NaCl salt (Fisher Scientific) in 100 mL water. The NaCl/NaBr solution was a mixture of 20% (by weight) NaCl and 0.08% (by weight) NaBr. After the reaction tube was coated with halide solution, it was inserted into the flow tube, cooled, and evacuated to a pressure of 1−2 Torr. This procedure created a halide-ice film that completely covered the inner surface of the reaction tube. Films were less than 0.1 mm thick and smooth to the eye. Although not measured directly, we expect that halide-ice films were smooth on the molecular level as well. On the basis of previous results for gas uptakes onto ice films made using a similar procedure,[25] we infer that halide-ice surfaces used in these experiments were smooth on a molecular scale.

$H^+$ concentrations in bromide-ice films were altered by changing the pH of NaBr solutions with which they were made. Known amounts of $H_2SO_4$ (Fisher Scientific, 34 N), HBr (Aldrich Chemical, 48%), and NaOH (Fisher Scientific, 1 N) were added to NaBr solutions to adjust their pH to 2, 4, and 10, respectively. pH values were confirmed by measuring the solutions with a pH meter.

The reaction tube was kept at a constant temperature by a bath of heat transfer fluid (Syltherm XLT, Dow Chemical) that circulated through a jacket surrounding the flow tube. To inhibit net evaporation of the halide-ice film during an experiment, water was added to the flow tube by bubbling helium carrier gas through a water trap at a rate of 100 standard cubic centimeters per minute (sccm). Water partial pressures were adjusted to match within 10% the water vapor pressure of the halide-ice film at the temperature of the experiment. Total helium carrier gas flow rate through the flow tube was 265−380 sccm.

Commercially available $Cl_2$ (Matheson, 99.9%) was used without purification in a mixture of UHP helium (Linox Gas Tech, 99.999%) and 1% $Cl_2$ by volume. Average $Cl_2$ concentrations in the flow tube ranged from $8 \times 10^{11}$ to $3 \times 10^{12}$ molecules/cm$^3$, as calculated from the change in pressure of the He−$Cl_2$ mixture with respect to time during an experiment. HOCl and BrCl were synthesized in the absence of excess $Cl_2$ so that their chemistry could be studied without interference. HOCl was made by slowly adding 200 mL NaOCl (Aldrich Chemical, 13% active chlorine) to a solution of 40 g of $MgSO_4{\bullet}7H_2O$ salt (Fisher Scientific) dissolved in 100 mL water. The HOCl solution was purified by vacuum distillation, and it was stable for up to one month when stored in the dark at 273 K.[26,27] During an experiment, gaseous HOCl was introduced into the flow tube by bubbling helium at a rate of 15−25 sccm through the aqueous HOCl solution at 273 K. Analysis of HOCl absorption at 240 nm indicates that HOCl concentration in the flow tube was approximately $3 \times 10^{12}$ molecules/cm$^3$. Gas flows contained less than 10−15% $Cl_2$ as confirmed by mass spectroscopic analysis. Gas-phase BrCl was made from a mixture of $Cl_2$ and $Br_2$ (Fisher Scientific). $Br_2$ was purified via several freeze−pump−thaw cycles at 77 K and then introduced into a glass bulb in approximately 5 times excess of $Cl_2$. The bulb was pressurized to 760 Torr by addition of helium, and this mixture was allowed to reach equilibrium over 48 h. The final BrCl concentration was calculated according to:[28]

$$Br_2 + Cl_2 \leftrightarrow 2BrCl \qquad K^{298} = 7.63 \qquad \text{(R6)}$$

BrCl concentration in the flow tube averaged $4 \times 10^{12}$ molecules/cm$^3$, as calculated from reaction R6 and the change in pressure of the He−BrCl−$Br_2$ mixture with respect to time during an experiment. Mass spectrometer measurements confirmed that the final experimental mixture contained less than 10% $Cl_2$.

Time-dependent kinetic measurements were made by establishing a flow of reactant $Cl_2$, HOCl, or BrCl gas through a movable injector that was pushed into the flow tube past the end of a halide-ice film. During an experiment, the movable

**TABLE 1: Reaction Probabilities for Reactions with Bromide−Ice Films at 233 K**[a]

| $[Br^-]$ (wt %) | $\gamma Cl_2$ | $\gamma HOCl$ | $\gamma BrCl$ | pH |
|---|---|---|---|---|
| 0.01 | 0.011 | | | 7 |
| 0.05 | 0.017 | | | 7 |
| 0.1 | 0.028 | 0.051 | 0.018 | 2 |
| 0.1 | | 0.011 | | 4 |
| 0.1 | 0.025 | 0.017 | 0.018 | 7 |
| 0.1 | | 0.014 | | 10 |
| 0.5 | 0.048 | 0.015 | | 7 |
| 1 | 0.060 | 0.019 | 0.042 | 7 |
| 1.5 | 0.075 | | | 7 |
| 2 | 0.085 | | | 7 |
| 3 | 0.097 | | | 7 |
| 5 | 0.098 | | | 7 |

[a] Average standard deviations are listed in the text.

injector was pulled back incrementally in order to expose individual sections of the ice film to the reactant gas. In each experiment, increasingly larger amounts of the halide-ice film were sequentially exposed. Decay of reactant signal and formation of products were monitored by the mass spectrometer, located downstream from the flow tube. Gas-phase $Cl_2$, HOCl, BrCl, and $Br_2$ were measured as parent ions at masses 70, 52, 116, and 160, respectively.

Gas-surface reaction probabilities ($\gamma$) were calculated from the first-order rate constants for reaction of $Cl_2$, HOCl, or BrCl with halide-ice films. In these calculations, we assumed that halide-ice film surfaces were smooth. To account for reactant concentration gradients in the flow tube that arise when there is substantial reactant wall loss, the observed first order decays were corrected by the method of Brown.[29] In all cases, diffusion coefficients were calculated for a He−$H_2O$ mixture as described by Hanson and Ravishankara.[30,31]

Observed rate constants were first order over the entire range of reactant gas concentrations used in these experiments. Because we were not able to conduct laboratory flow tube studies using the very low reactant gas concentrations representative of the troposphere, we cannot be absolutely certain that rate constants are first order in this regime. However, if the reactions did not follow first-order kinetics at low reactant gas concentrations, we should have seen evidence of the deviation at the high reactant gas concentrations used in these experiments. Thus, even though $Cl_2$, HOCl, and BrCl concentrations in this study were significantly higher than in the troposphere, kinetic data presented here should be relevant to Arctic chemistry.

Uncertainty in reaction probability values arises mainly from variations in the ice film surface from experiment to experiment. Reaction probabilities from a series of experiments run under the same conditions can vary to some degree, thus each reported reaction probability listed in Table 1 is the mean of values from 3 to 6 identical experiments. Average standard deviations for reaction probabilities listed in Table 1 are ±33% for reactions with $Cl_2$, ±27% for reactions with HOCl, and ±11% for reactions with BrCl. In general, individual standard deviations range from ±10−30% for $0.01 \leq \gamma \leq 0.07$, and ±40−80% for $\gamma > 0.07$.

$Br_2$ and BrCl mass spectrometer signals were calibrated in order to estimate product yields for reactions of $Cl_2$ and HOCl. BrCl and $Br_2$ flow tube concentrations were calculated from reaction R6 and the change in pressure of the He−BrCl−$Br_2$ mixture with respect to time during an experiment. BrCl and $Br_2$ flow tube concentrations were correlated with their mass spectrometer signals measured when the movable injector was first pulled back. These ratios were used to calculate BrCl and $Br_2$ yields in reactions of $Cl_2$ and HOCl with bromide-ice films at 233 K and with chloride/bromide-ice films at 248 K.

## Results and Discussion

**1. Reactions with Bromide-Ice Surfaces at 233 K.** The first step in this study involved working with ice films that contained only bromide. Experiments were conducted at 233 K; typical temperatures in the springtime Arctic boundary layer range from 230 to 250 K.

*1a. Reactions with $Cl_2$.* Representative data for the reaction of $Cl_2$ gas with a bromide-ice film at 233 K are shown in Figure 2a. These experiments examined the reactions:

$$Cl_2 + Br^- \rightarrow BrCl + Cl^- \qquad (R7)$$

$$BrCl + Br^- \rightarrow Br_2 + Cl^- \qquad (R2)$$

Reactant and product signals are plotted versus injector position in centimeters and time in seconds in Figure 2a. The movable injector was pulled back incrementally during an experiment, exposing increasingly larger sections of the bromide-ice film. In a typical experiment, the injector was pulled back to positions of 1, 3, 6, 10, and 15 cm, which exposed 1, 2, 3, 4, and 5 cm of fresh ice film, respectively. For example, in the experiment shown in Figure 2a, the injector was moved from 3 to 6 cm at 220 s, and 3 cm of fresh bromide-ice surface were exposed. Each time the injector was pulled back, $Cl_2$ reacted with bromide in the ice film to produce $Br_2$ and a very small amount of intermediate product BrCl. The BrCl signal has been offset for clarity and magnified 10 times so that it lies on the same scale as the $Cl_2$ and $Br_2$ signals. Time dependent loss and recovery of the $Cl_2$ signal were due to depletion of bromide at the surface of the ice film.

Note that data presented here are different from those of traditional gas-surface reaction probability studies because bromide on the ice surface was consumed during the course of an experiment. Each time the movable injector was pulled back, the $Cl_2$ signal decreased rapidly, and the product signals increased as $Cl_2$ reacted with bromide on the freshly exposed ice film to produce $Br_2$ and BrCl. As greater amounts of bromide were lost to reaction, the $Cl_2$ signal gradually recovered while the product signals decreased to background values. Consequently, reversible behavior was not observed: when the movable injector was pushed in, there was no concurrent increase in $Cl_2$ signal.

In these experiments, reaction of $Cl_2$ with a fresh bromide-ice surface followed first-order kinetics. However, due to the atypical nature of this heterogeneous chemistry, first-order rate constants were not extracted in the usual manner. In contrast to the common method of plotting reactant signal as a function of injector position, Figure 2b shows the change in $Cl_2$ “signal ratio” with increasing “reactive ice surface” size for the experiment shown in Figure 2a. The slope of the best fit line through the data yields the first-order rate constant. “Signal ratio” is defined as the value of the $Cl_2$ signal immediately after the injector was pulled back divided by the value of the $Cl_2$ signal immediately before the injector was pulled back. Thus, “signal ratio” represents the instantaneous change in $Cl_2$ signal as the movable injector was pulled back and $Cl_2$ reacted with bromide on a fresh ice surface. It is not appropriate to plot the absolute value of the $Cl_2$ signal because it gradually increased back to its original value as bromide reacted away during an experiment. “Reactive ice surface” is the amount of fresh bromide-ice surface that was exposed by the movable injector

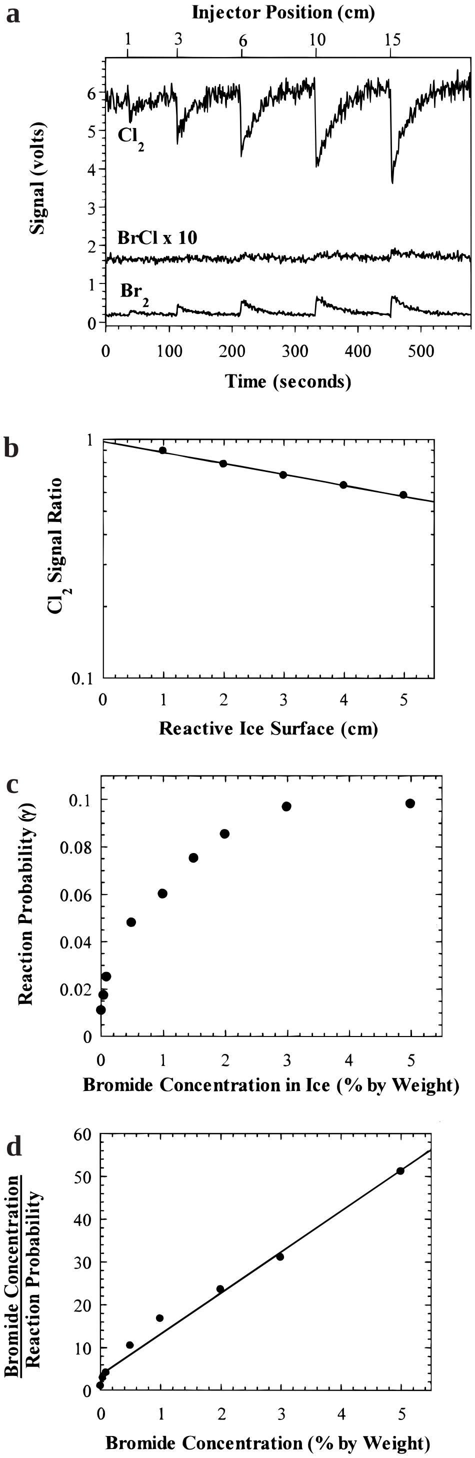

**Figure 2.** (a) Representative data for the reaction of $Cl_2$ with a 0.1% bromide-ice film at 233 K, pH 7. During the experiment, the movable injector was pulled back incrementally, exposing increasingly larger sections of the bromide-ice film to $Cl_2$. Each time the injector was pulled back, $Cl_2$ reacted with bromide in the ice film to produce $Br_2$ and a very small amount of BrCl. Time dependent loss and recovery of the $Cl_2$ signal were due to depletion of bromide at the ice surface. The BrCl signal is offset for clarity and magnified 10 times so that it lies on the same scale as $Cl_2$ and $Br_2$. (b) $Cl_2$ "signal ratio" as a function of "reactive ice surface" for the experiment shown in Figure 2a. The slope of the best fit line through the data yields the first-order rate constant. "Signal ratio" and "reactive ice surface" are defined in the text. These values are used because the bromide-ice surface was deactivated each time the movable injector was pulled back. (c) Reaction probability ($\gamma$) as a function of bromide concentration in ice for reactions of $Cl_2$ with bromide-ice films at 233 K, pH 7. (d) $[Br^-]/\gamma$ as a function of $[Br^-]$ for the $Cl_2$ data reported in Table 1. The correlation coefficient for the best fit line through the data is 0.99.

as it was pulled back. This value is used instead of absolute injector position because the bromide-ice film was deactivated each time the movable injector was pulled back. For example, in Figure 2a, the injector was moved from 6 to 10 cm at 340 s, and 4 cm of fresh bromide-ice surface were exposed. The $Cl_2$ signal dropped from approximately 6.2 V to 4.1 V, yielding a "signal ratio" of 0.64; this value is plotted versus 4 cm of "reactive ice surface" in Figure 2b.

In this manner, reaction probabilities were calculated for bromide concentrations ranging from 0.01% to 5% bromide in ice. Results shown in Figure 2c and Table 1 indicate that there is a direct relationship between higher reaction probability and larger amounts of bromide in an ice film, up to bromide concentrations of approximately 3%. Reaction probability appears to level off to a constant value at bromide concentrations $\geq$3%. As discussed at the end of this section, it seems likely that factors other than bromide concentration control reaction rate at bromide concentrations $\geq$3%.

The $Cl_2$ reaction probability for interaction with a 0.1% bromide-ice film at pH 2 was also determined. The value, listed in Table 1, is nearly identical to that for reaction with a 0.1% bromide-ice film at pH 7. This result demonstrates that $H^+$ concentration does not affect the rate of reaction R7.

Although we did not measure the spatial distribution of bromide in the film, phase transition studies of salt solutions suggest that bromide ions were concentrated at the ice surface. As a salt solution freezes, the rate at which an anion or cation is incorporated into the ice is determined by its distribution coefficient, which is a measure of the distortion that the solute imposes on the molecular arrangement in the solid ice. For ionic solutes in water, the distribution coefficient is very small.[32] Therefore, as a salt solution freezes, pure ice forms first, and the surrounding brine becomes increasingly enriched. This segregation continues as temperatures decrease to the eutectic temperature, at which point only a very small amount of enriched salt solution remains in the liquid phase on the ice surface. Below the eutectic temperature, the salt solution freezes. Thus, at 233 K, phase transition theory predicts that the freezing process will concentrate bromide ions at the surfaces of the halide-ice films used in this study.

Our experimental results support the idea that a majority of the bromide was located at the ice surface. The total number of $Cl_2$ molecules that reacted with the bromide-ice film each time the movable injector was pulled back can be calculated from integration of the corresponding $Cl_2$ signal peak. This value can be compared to the amount of bromide in the related section of exposed film to determine the fraction of bromide ions that reacted with $Cl_2$. Multiple analyses indicate that the number of bromide ions needed to react with the quantity of $Cl_2$ lost was a large fraction of the total amount of bromide in the ice film. Within a factor of 5, all of the bromide ions in the ice film were accessible by $Cl_2$. This reaction was too fast for $Cl_2$ to have diffused very far into the bulk ice. Therefore, bromide ions were not homogeneously mixed throughout the depth of the ice film, but instead were concentrated at the ice surface where they were available for reaction.

The phase of the bromide-ice reactive interface can be inferred from analysis of the kinetic data. In these experiments, it is unlikely that $Cl_2$ reacted with aqueous bromide in a pure liquid layer on the ice film surface. The steady-state reaction probability for $Cl_2$ loss from the gas-phase through a pseudo first-order reaction in a liquid is given by:[33]

$$\gamma \approx \frac{4RTH\sqrt{Dk^{\mathrm{I}}}}{c} \tag{E1}$$

where $\gamma$ is the reaction probability, $R$ is the ideal gas constant, $T$ is temperature, $c$ is the mean molecular speed of gas-phase $Cl_2$, and $H$ and $D$ are the Henry's law coefficient and liquid-phase diffusion coefficient, respectively, for $Cl_2$ in water. For first-order kinetics, $k^{\mathrm{I}} = k^{\mathrm{II}}[\mathrm{Br}^-]_l$, where $k^{\mathrm{II}}$ is the second-order liquid-phase rate constant and $[\mathrm{Br}^-]_l$ is the liquid-phase concentration of bromide. Consequently, $Cl_2$ reaction probability is linearly proportional to the square root of bromide concentration for a pure liquid-phase reaction. However, there is not a linear relationship between $Cl_2$ reaction probability and the square root of bromide concentration for the data in these experiments. This result implies that reaction R7 does not occur in a pure liquid phase on the surface of a bromide-ice film at 233 K.

It is more likely that the bromide-ice reactive interface is a solid, since the kinetic data can be fit to the Eley–Rideal mechanism for reaction of a gas-phase molecule ($Cl_2$) colliding with a compound ($\mathrm{Br}^-$) adsorbed on a solid surface. This mechanism is a reasonable approximation for reaction R7, assuming very little $Cl_2$ adsorbed onto the ice surface. If a significant fraction of $Cl_2$ molecules were taken up by the bromide-ice surface, then reaction R7 would more closely follow the Langmuir–Hinshelwood mechanism, which describes reaction between two adsorbed species at neighboring sites on a surface. However, Hanson and Ravishankara saw no loss of $Cl_2$ on an ice surface at 200 K,[18] and this behavior is not likely to change significantly over 33 K. It is fair to assume that very little $Cl_2$ adsorbed onto the ice surface and that the mechanism of reaction R7 most closely resembles the Eley–Rideal model.

The reaction rate for an Eley–Rideal mechanism in terms of reaction R7 is described by:[34]

$$-\frac{\mathrm{d}P_{\mathrm{Cl}_2}}{\mathrm{d}t} = k_s\, S_0\, \theta_{\mathrm{Br}^-}\, P_{\mathrm{Cl}_2} \tag{E2}$$

where $k_s$ is the first-order rate constant for loss of gas-phase $Cl_2$ at the bromide-ice surface, $S_0$ is the total number of sites available for bromide on the ice surface, $\theta_{\mathrm{Br}^-}$ is an expression for the coverage of bromide on the ice surface, and $P_{Cl_2}$ is the partial pressure of $Cl_2$. The loss of gas-phase $Cl_2$ with respect to time in the flow tube system is expressed by:[35]

$$-\frac{\mathrm{d}P_{\mathrm{Cl}_2}}{\mathrm{d}t} = \frac{\gamma c}{2r} P_{\mathrm{Cl}_2} \tag{E3}$$

where $\gamma$ is the reaction probability, $r$ is the radius of the flow tube, and $c$ is the mean molecular speed of gas-phase $Cl_2$. Setting equation E2 equal to equation E3 and reducing yields:

$$\gamma = \left(\frac{2rk_s}{c} S_0\right)\theta_{\mathrm{Br}^-} = \gamma_0 \theta_{\mathrm{Br}^-} = \gamma_0\left(\frac{K_{\mathrm{Br}^-}[\mathrm{Br}^-]}{1 + K_{\mathrm{Br}^-}[\mathrm{Br}^-]}\right) \tag{E4}$$

where $\gamma_0$ is the reaction probability for reaction of $Cl_2$ with bromide on an ice surface that is saturated with bromide, and $\theta_{\mathrm{Br}^-}$ is expressed as a Langmuir adsorption isotherm for bromide on the ice surface with $K_{\mathrm{Br}^-}$ representing the equilibrium constant for bromide adsorption. Since phase transition theory and our experimental results indicate that most of the bromide in the ice was concentrated at the surface of the film, it is reasonable to approximate bromide coverage with the Langmuir isotherm. Rearranging equation E4 to a linear form gives:

$$\frac{[\mathrm{Br}^-]}{\gamma} = \frac{[\mathrm{Br}^-]}{\gamma_0} + \frac{1}{K_{\mathrm{Br}^-}\gamma_0} \tag{E5}$$

As expressed by equation E5, the Eley–Rideal mechanism for reaction of gas-phase $Cl_2$ with bromide on a solid ice surface predicts that a plot of $[\mathrm{Br}^-]/\gamma$ versus $[\mathrm{Br}^-]$ will yield a straight line with a slope equal to $1/\gamma_0$. Figure 2d shows that for $Cl_2$ data reported in Table 1, $[\mathrm{Br}^-]/\gamma$ is in fact a linear function of $[\mathrm{Br}^-]$, with a correlation coefficient of 0.99 for the best fit line through the data. On the basis of this analysis, our experimental data are much more consistent with a solid bromide-ice reactive surface rather than a pure liquid layer at 233 K.

The slope of the best fit line in Figure 2d gives a value of 0.1 for $\gamma_0$, which represents the theoretical $\gamma$ for reaction of $Cl_2$ with a bromide-ice film that is saturated with bromide. In Figure 2c, reaction probabilities approach a constant value of 0.1 at bromide concentrations of approximately 3% and greater. Taken together, these results imply that at 233 K, an ice surface is completely saturated with bromide at concentrations $\geq 3\%$, and that under these conditions, at most 1 in 10 collisions of $Cl_2$ with the bromide-ice surface result in reaction. In this regime, increasing the bromide concentration in the ice film does not increase the reaction probability. Instead, maximum reaction probability may be set by parameters such as the physical arrangement of the reacting species or their extent of hydration. For example, it is possible that the reaction probability is limited to 0.1 because only 10% of individual $Cl_2$ molecules strike the bromide-ice surface in the correct configuration for reaction to occur, assuming every properly aligned collision leads to reaction.

In conclusion, it appears that for the heterogeneous reactions of $Cl_2$ with bromide-ice films, reaction probability increases with increasing bromide concentration in the ice film. However, at approximately 3% bromide concentration, the ice surface is completely covered with bromide ions. At this point, the maximum reaction probability is 0.1, and any increase in bromide concentration in the ice film above approximately 3% does not result in a higher reaction probability.

*1b. Reactions with HOCl.* Representative data for the reaction of HOCl gas with a bromide-ice film at 233 K are shown in Figure 3a. These experiments examined the reactions:

$$\mathrm{HOCl} + \mathrm{Br}^- + \mathrm{H}^+ \rightarrow \mathrm{BrCl} + \mathrm{H_2O} \tag{R8}$$

$$\mathrm{BrCl} + \mathrm{Br}^- \rightarrow \mathrm{Br_2} + \mathrm{Cl}^- \tag{R2}$$

The data look very similar to results from the $Cl_2$ experiments described in section 1a. HOCl reacted with bromide in the ice film to form $Br_2$ and a very small amount of BrCl. As was the case with $Cl_2$, time dependent loss and recovery of the HOCl signal were due to depletion of bromide at the ice film surface, and the reactions followed first-order kinetics.

To examine the importance of $\mathrm{H}^+$ in reaction R8, experiments were conducted using ice films that contained a constant bromide concentration of 0.1% but varying hydrogen ion concentrations. HOCl reaction probabilities were calculated in the same manner as described for $Cl_2$ in section 1a. Results are shown in Figure 3b and Table 1 for films made from NaBr solutions of pH 2, 4, 7, and 10. In experiments with films made from solutions of pH 4, 7, and 10, HOCl reaction probabilities are approximately equal. However, the value at pH 2 is 5 times greater, implying that the rate of reaction R8 is significantly faster on an acidic surface with a low pH. In addition, HOCl reaction probabilities for 0.5% and 1% bromide-ice films at

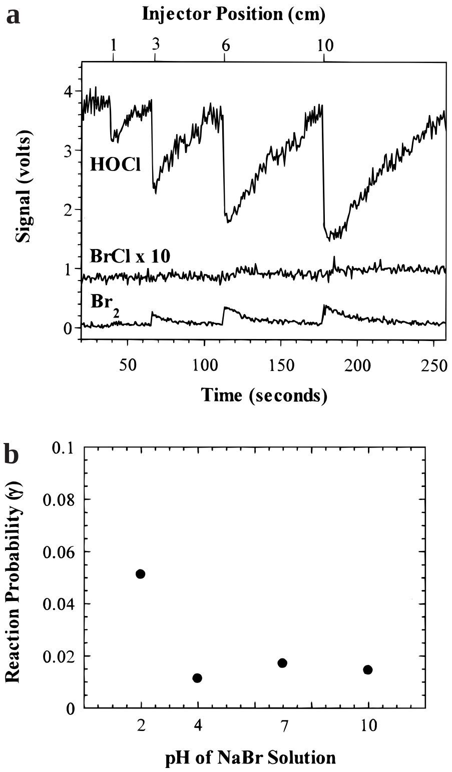

**Figure 3.** (a) Representative data for the reaction of HOCl with a 0.1% bromide-ice film at 233 K and pH 7. Time dependent loss and recovery of the HOCl signal were due to depletion of bromide at the ice surface, as for $Cl_2$ in Figure 2a. The BrCl signal is offset for clarity and magnified 10 times so that it lies on the same scale as HOCl and $Br_2$. (b) Reaction probability ($\gamma$) as a function of pH for reactions of HOCl with 0.1% bromide-ice films at 233 K. 0.1% bromide-ice films were made from NaBr solutions with varying pH as described in the text.

pH 7 are essentially equivalent to values for 0.1% bromide-ice films at pH 4, 7, and 10. This result indicates that in contrast to reactions with $Cl_2$, HOCl reaction rate does not increase with increasing bromide concentration in ice. Reaction R8 is limited by $H^+$ concentration, not bromide concentration, at pH values greater than 2.

*1c. Reactions with BrCl.* The chemistry of BrCl formation in the flow tube was investigated in order to interpret fully results from experiments with $Cl_2$ and HOCl. The reaction of gas-phase $Cl_2$ or HOCl with bromide on an ice film may be considered as a series of consecutive reactions:

$$Cl_{2(g)} + Br^- \rightarrow BrCl_{(a)} + Cl^- \qquad (R7)$$

$$HOCl_{(g)} + Br^- + H^+ \rightarrow BrCl_{(a)} + H_2O \qquad (R8)$$

$$BrCl_{(a)} + Br^- \rightarrow Br_{2(g)} + Cl^- \qquad (R2)$$

$$BrCl_{(a)} \rightarrow BrCl_{(g)} \qquad (R9)$$

$$BrCl_{(g)} + Br^- \rightarrow Br_{2(g)} + Cl^- \qquad (R2')$$

where the subscript (a) represents molecules adsorbed on the ice film, and the subscript (g) represents molecules that are in the gas phase. The concentration of $BrCl_{(a)}$ is set by production in reaction R7 or R8 and loss via reactions R2 and R9. During the course of an experiment, reactions R7 or R8, R2 and R2′ are in competition for bromide. On a short time scale, the main product of reactions R7 or R8 and R2 is expected to be gas-phase $Br_2$ because these reactions are not limited by bromide concentration when the movable injector is first pulled back to expose fresh bromide-ice surface. As bromide is depleted, however, reaction R9 becomes competitive, and $BrCl_{(a)}$ may degas from the ice surface before it can react via reaction R2.

**TABLE 2: Upper Limits to Reaction Probabilities for Reactions with Chloride−Ice Films at 233 K**

| $[Cl^-]$ (wt %) | $\gamma Cl_2$ | $\gamma$HOCl | pH |
|---|---|---|---|
| 0.1 | <0.0019 | <0.0047 | 7 |
| 1 | <0.0010 | <0.0042 | 7 |

Because the concentration of gas-phase BrCl in the flow tube is limited by loss via reaction R2′, it is impossible to determine the relative yields of gas-phase $Br_2$ and BrCl from reactions R7 or R8 and R2 without knowing the reaction probability for reaction R2′. Very small BrCl mass spectrometer signals in Figures 2a and 3a may indicate that reaction R9 is too slow to produce significant amounts of gas-phase BrCl. On the other hand, because of the competition for bromide at the ice surface, BrCl mass spectrometer signals would also be small if reaction R2′ were very fast. If reaction R2′ were faster than reaction R7 or R8, then a significant fraction of gas-phase BrCl produced by reaction R9 might react away before it could be detected in the mass spectrometer.

To determine the fate of $BrCl_{(a)}$ in the flow tube, reaction probabilities were measured for reaction R2′, the reaction of gas-phase BrCl with bromide-ice surfaces at 233 K. Results are listed in Table 1. At pH 7, BrCl reaction probabilities are significantly less than values for corresponding experiments with $Cl_2$, and the value for 0.1% bromide-ice is approximately equal to that for the analogous experiment with HOCl. In addition, the BrCl reaction probability for 0.1% bromide-ice at pH 2 is much less than the value for the same experiment with HOCl. Therefore, at 233 K, $BrCl_{(g)}$ reacts with bromide on the ice surface more slowly than $Cl_{2(g)}$ and at the same rate or slower than $HOCl_{(g)}$, depending on pH. It is fair to conclude that very little BrCl degassed from the bromide-ice surface in the flow tube experiments; most of the $BrCl_{(a)}$ formed in reaction R7 or R8 stayed on the ice surface and reacted directly with bromide via reaction R2. Thus, for these reactions, small BrCl mass spectrometer signals reflect the fact that reaction R9 is slow.

Note that BrCl reaction probabilities for reaction with 0.1% bromide-ice at pH 2 and pH 7 are nearly identical, which demonstrates that the effect of increasing rate with decreasing pH is unique to the HOCl reaction.

**2. Reactions with Chloride-Ice Surfaces at 233 K.** The next step in the study was to examine interactions of gas-phase $Cl_2$ and HOCl with ice surfaces that contained only chloride. At 233 K and pH 7, no reaction between $Cl_2$ or HOCl and chloride-ice films was observed. Conservative estimates of the upper limit to observable reaction probabilities are listed in Table 2, and they are significantly less than values for corresponding reactions with bromide-ice films.

The absence of a reaction was not surprising in the case of $Cl_2$, but it was unexpected for HOCl. The reaction of HOCl with a chloride-ice film to form $Cl_2$ seemed possible via

$$HOCl + Cl^- + H^+ \rightarrow Cl_2 + H_2O \qquad (R10)$$

Failure to observe a reaction may be related to the fact that the rate constant of reaction R10 in aqueous solution is 100 times smaller than that of reaction R8.[36] It is also possible that reaction R10 was limited by $H^+$ concentration at pH 7.

**TABLE 3: Reaction Probabilities for Reactions with Chloride/Bromide−Ice Films at pH 7[a]**

| $T$ (K) | $\gamma Cl_2$ | $\gamma$HOCl |
|---|---|---|
| 233 | <0.0020 | <0.0042 |
| 248 | 0.0048 | 0.013 |

[a] Films contained 20% chloride/0.08% bromide by weight as described in the text.

**3. Reactions with Chloride/Bromide-Ice Surfaces.** These experiments were designed to simulate reactions of $Cl_2$ and HOCl with Arctic sea ice. To replicate frozen seawater surfaces in the laboratory, ice films containing both chloride and bromide were made from a NaCl/NaBr solution as described in the Experimental section. Halide concentrations in the experimental NaCl/NaBr solution were approximately 10 times greater than in natural seawater so that there was sufficient bromide in the ice film for reaction with $Cl_2$ and HOCl. Despite being made from a concentrated NaCl/NaBr solution, laboratory chloride/bromide-ice films were reasonable surrogates for natural sea ice surfaces. Halide concentrations in Arctic sea ice are probably much higher than in seawater due to enhancement from the ice freezing process and from deposition of sea salt aerosols. In the atmosphere, deliquescent sea salt aerosols become enriched in chloride and bromide as the relative humidity falls below 100%.

*3a. Temperature = 233 K.* At 233 K, there was no reaction between the chloride/bromide-ice film and either $Cl_2$ or HOCl. Conservative estimates of the upper limit to observable reaction probabilities are listed in Table 3. Absence of a reaction was surprising because the amount of bromide present in the chloride/bromide-ice film was sufficient for reaction in corresponding experiments with ice films that contained only bromide. For example, reaction probabilities for 0.1% bromide-ice films at pH 7 are significantly larger than the estimated upper limit reaction probabilities for chloride/bromide-ice films at 233 K. The difference in reactivity between the two types of halide-ice films may be due to the large amount of unreactive chloride in the chloride/bromide-ice film. It is possible that the reactive ice surface was saturated by the addition of almost 300 times more chloride than bromide. At 233 K, based on comparison of reaction probability values, there was less bromide on the reactive surface of the chloride/bromide ice film than on the 0.1% bromide-ice film, even though both films were made from solutions containing approximately the same amount of NaBr. Future studies are necessary in order to elucidate the composition of halide-ice surfaces.

*3b. Temperature = 248 K.* Laboratory experiments were also conducted at 248 K to investigate the reactivity of chloride/bromide-ice films near the upper limit of typical temperatures in the springtime Arctic boundary layer. In contrast to results at 233 K, both $Cl_2$ and HOCl reacted with a chloride/bromide-ice film at 248 K. Representative data from an experiment with $Cl_2$ are shown in Figure 4. Mass spectrometer data look similar to results shown in Figures 2a and 3a for reactions of $Cl_2$ and HOCl with bromide-ice films at 233 K. In the experiment shown in Figure 4, $Cl_2$ reacted with bromide in the chloride/bromide-ice film to produce $Br_2$ and a very small amount of BrCl. As in experiments with bromide-ice films, time dependent loss and recovery of the $Cl_2$ signal were due to depletion of bromide at the ice surface, and the reactions followed first-order kinetics.

Reaction probabilities for experiments with chloride/bromide-ice films at 248 K are listed in Table 3. These values are significantly larger than upper limit reaction probability estimates for experiments with chloride/bromide-ice films at 233 K. The difference in chloride/bromide-ice film reactivity at 248 K versus 233 K is probably related to the freezing process of salt solutions as described in section 1a. 248 K is between the eutectic temperatures of pure NaCl (252 K) and pure NaBr (245 K). As the experimental NaCl/NaBr solution froze to make a chloride/bromide-ice film, ice formed first, and the remaining solution became increasingly enriched in salt. Below 252 K, phase transition theory predicts that the NaCl solution was completely frozen while a small amount of enriched NaBr solution remained liquid. Consequently, it is likely that at the experimental temperature of 248 K, a small amount of concentrated bromide was in solution and available for reaction on the ice film surface. The chloride/bromide-ice surface at 248 K was clearly more reactive than at 233 K, when NaCl and NaBr solutions were both completely frozen.

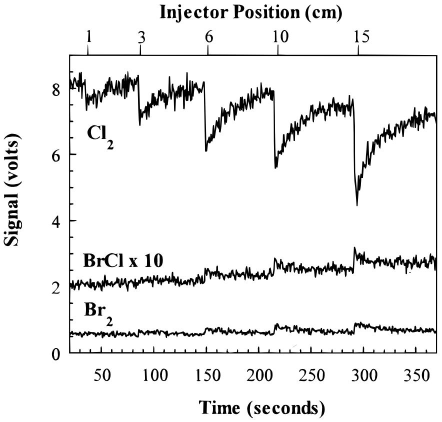

**Figure 4.** Representative data for the reaction of $Cl_2$ with a chloride/bromide-ice film at 248 K. The composition of the chloride/bromide-ice film is defined in the text. Time dependent loss and recovery of the $Cl_2$ signal were due to depletion of bromide at the ice surface, as in Figure 2a. The BrCl signal is offset for clarity and magnified 10 times so that it lies on the same scale as $Cl_2$ and $Br_2$.

Rates for reaction of $Cl_2$ and HOCl with chloride/bromide-ice films at 248 K are slower than in corresponding experiments with ice films that contained only bromide. For example, the $Cl_2$ reaction probability for a 0.1% bromide-ice film at pH 7 is 10 times greater than that for a chloride/bromide-ice film at 248 K. In addition, the HOCl reaction probability for a 0.1% bromide-ice film at pH 2 is 5 times greater than the value for a chloride/bromide-ice film at 248 K. These results confirm that addition of chloride physically changed the reactive surface composition of the halide-ice films. On the basis of reaction probability values, there was significantly less bromide concentrated on the surface of a 20% NaCl/0.08% NaBr solution frozen at 248 K than on the surface of a 0.1% NaBr solution frozen at 233 K.

In summary, our experimental data imply that as seawater freezes, chloride and bromide ions do not remain homogeneously mixed throughout the bulk ice, but rather concentrate at the surface in a way that is dependent on composition and temperature. Thus, it is likely that the chemical composition and phase of natural sea ice surfaces, modified by temperature, are critical factors controlling heterogeneous reaction rates with $Cl_2$ and HOCl in the Arctic troposphere.

**4. Product Yields.** To evaluate the impact of $Cl_2$ and HOCl reactions with sea ice in the Arctic, it is necessary to determine yields of gas-phase $Br_2$ and BrCl from reactions studied in the laboratory. Product yields were estimated in $Cl_2$ and HOCl reactions with bromide-ice films at 233 K and with chloride/bromide-ice films at 248 K as described in the Experimental section. In all cases, gas-phase $Br_2$ was the main product. For reactions with $Cl_2$, 1−2% of the yield was BrCl and 98−99% was $Br_2$. In HOCl reactions, yields were 3% or less BrCl and 97% or more $Br_2$.

Results from section 1c demonstrate that BrCl product yields reported here are accurate reflections of the amount of BrCl that degassed from the halide-ice surface. $BrCl_{(a)}$ produced gas-phase $Br_2$ via reaction R2 faster than it could degas into the flow tube via reaction R9. Very small BrCl signals observed in the mass spectrometer reflected the fact that little $BrCl_{(a)}$ degassed from the halide-ice surface. This distinction is important for extrapolation of laboratory results to the Arctic troposphere.

On the basis of the stoichiometry of reactions R7 or R8 and R2, formation of one gas-phase $Br_2$ molecule was expected for every $Cl_2$ or HOCl molecule lost. However, we observed 50% less gas-phase $Br_2$ than predicted from the number of $Cl_2$ or HOCl molecules lost in flow tube experiments. Adsorption of $Cl_2$ and HOCl on the ice surface should have been minimal in these experiments, since we saw no reversible uptake at 233 K when $Cl_2$ and HOCl were exposed to an ice film that did not contain bromide. Therefore, it is reasonable to conclude that $Cl_2$ and HOCl were not taken up by the ice surface but instead were lost by reaction with bromide to produce $BrCl_{(a)}$ via reaction R7 or R8. Furthermore, it is clear that 97% or more of the $BrCl_{(a)}$ produced via reactions R7 and R8 formed gas-phase $Br_2$. Consequently, the number of $Cl_2$ or HOCl molecules lost in these experiments should have led to formation of approximately the same amount of $Br_2$ gas. Since only half of the expected $Br_2$ was detected in the mass spectrometer, the difference must have remained adsorbed on the bromide-ice surface. A similar phenomenon was observed by Chu and Chu[19] and by Hanson and Ravishankara,[18] who attributed the variance in $Br_2$ signal to mass discrimination in their mass spectrometer.

The relative product yields in the $Cl_2$ and HOCl experiments presented here are consistent with results from analogous studies by other researchers. Mochida et al.[17] calculated a $Br_2$ yield of 92±8% in the reaction of $Cl_2$ with solid sea salts at ambient temperature in a Knudsen cell reactor. For the reaction of $Cl_2$ with HBr on an ice surface at 220 K, Hanson and Ravishankara[18] did not detect the formation of any gas-phase BrCl. In a similar manner, Chu and Chu[19] observed only very small gas-phase BrCl production in the reaction of HOCl with HBr on ice films at 189 and 220 K.

## Atmospheric Implications

This study is the first attempt to identify which factors control the reactions of atmospheric $Cl_2$ and HOCl with sea ice surfaces in the Arctic boundary layer. Experiments reported here were run under conditions that were comparable to those in the Arctic, but not identical. It is impossible to completely duplicate natural sea ice surfaces in the laboratory because their composition is not well known. To date, there are no reported measurements of chloride, bromide, or hydrogen ion concentrations at the surface of frozen seawater, but Barrie and co-workers recently analyzed ionic components in Arctic snow.[37] Results indicate that in April, there are approximately $5 \times 10^{14}$ bromide ions/$cm^3$ of freshly fallen Arctic snow. This value can be compared to the bromide concentration on the surface of a 0.1% bromide-ice film used in this study, which contained $2 \times 10^{16}$ bromide ions/$cm^2$, assuming 1 mL of 0.1% NaBr solution was frozen over the entire inner wall of the reaction tube. The field studies are not directly applicable to our laboratory study because Barrie analyzed the entire snowpack, not just the surface layer. Nonetheless, the field results provide some frame of reference for comparison of our experimental conditions with those in the Arctic.

Currently, it is not apparent what chemical reactions produce active chlorine compounds in the boundary layer. $Cl_2$ formation has been observed from the photolysis of ozone in the presence of aqueous sea salt aerosols,[38] and this mechanism may be an important source of active chlorine in the Arctic. It is difficult to quantify the tropospheric impact of this process because the physical chemistry leading to $Cl_2$ formation is complex. For example, a recent study[39] shows that the reactions responsible for $Cl_2$ production on deliquescent NaCl aerosols do not occur in the bulk aqueous phase but instead are dominant at the air−water interface. As a further complication, there may be as yet unknown active chlorine sources in the lower atmosphere. Despite the fact that all their specific formation mechanisms have not been identified, field campaigns show that $Cl_2$ and HOCl are present in the troposphere at significant concentrations,[14,15] and it is of interest to investigate the chemistry which these compounds may promote.

Results from laboratory experiments presented here indicate that a number of variables control reactions of $Cl_2$ and HOCl with halide-ice surfaces, including temperature, bromide concentration, chloride concentration, and hydrogen ion concentration in ice. On the basis of calculated reaction probabilities with bromide-ice surfaces at 233 K and with chloride/bromide-ice surfaces at 248 K, $Cl_2$ and HOCl heterogeneous reactions may impact $O_3$ chemistry in the Arctic troposphere. Reactions between bromide-ice films and $Cl_2$ are faster in general, but at low pH, reaction with HOCl is just as rapid. In the springtime Arctic, it is likely that sea ice surfaces are acidic from deposition of “Arctic haze” sulfate aerosol. During $O_3$ loss events, field measurements confirm that high concentrations of sulfate aerosol are widespread in the troposphere.[40] Thus, conditions in the springtime boundary layer are such that heterogeneous reaction of both $Cl_2$ and HOCl with sea ice could contribute significantly to bromide oxidation. Future studies must focus on determination of the specific bromide, chloride, and hydrogen ion concentration in Arctic sea ice, and how these characteristics change with temperature. Until the physical and chemical composition of reactive Arctic sea ice surfaces are well defined, it is difficult to quantitatively define absolute heterogeneous reaction rates.

Nevertheless, we can use our experimental data to calculate a rough estimate of the amount of gas-phase $Br_2$ formed by reaction of $Cl_2$ and HOCl with sea ice at 248 K. The reaction rate for $Cl_2$ or HOCl loss on a sea ice surface is best represented by a dry deposition flux:[41]

$$F = \nu C \qquad \text{(E6)}$$

where $\nu$ is the vertical deposition velocity and $C$ is the gas-phase reactant concentration. The vertical deposition velocity is calculated for a neutrally stable atmosphere from a resistance-in-series model that incorporates $Cl_2$ or HOCl aerodynamic transport through the atmospheric surface layer, molecular diffusion to the ice surface, and loss by heterogeneous reaction.[42] Appropriate $Cl_2$ and HOCl concentrations for the springtime Arctic boundary layer are estimated from field measurements made at Alert, Northwest Territories during the Polar Sunrise Experiment 1995.[14] Results from this field campaign indicate that mixing ratios of “photolyzable chlorine” ($Cl_2$ or HOCl) averaged 10−20 ppt from early March to mid-April;[14] we take 10 ppt = $2.95 \times 10^8$ molecules/$cm^3$ as a lower estimate for the steady-state concentration of $Cl_2$ or HOCl in the springtime

Arctic troposphere. The dry deposition fluxes for $Cl_2$ and HOCl loss on a sea ice surface at 248 K are given by:

$$F_{Cl_2} = (0.606\ \mathrm{cm/s})(2.95 \times 10^8\ \mathrm{molecules/cm^3}) = 1.79 \times 10^8\ \mathrm{molecules/(cm^2\ s)} \quad (E7)$$

$$F_{HOCl} = (0.614\ \mathrm{cm/s})(2.95 \times 10^8\ \mathrm{molecules/cm^3}) = 1.81 \times 10^8\ \mathrm{molecules/(cm^2\ s)} \quad (E8)$$

These flux values represent the $Cl_2$ or HOCl reaction rate per $cm^2$ of sea ice per second, assuming the reaction probabilities reported in Table 3 for chloride/bromide-ice films at 248 K are representative of reactions with Arctic sea ice. Product yield analyses indicate that $Cl_2$ reactions produced at least 98% $Br_2$ and HOCl reactions produced at least 97% $Br_2$. However, experimental results show that only half of the $Br_2$ produced by these reactions degassed from the sea ice surface. Therefore, gas-phase $Br_2$ production rates are expressed by:

$$(1.79 \times 10^8\ \mathrm{molecules\ of\ Cl_2\ lost/(cm^2\ s)})(0.98)(0.95) = 8.76 \times 10^7\ \mathrm{molecules\ of\ Br_2/(cm^2\ s)} \quad (E9)$$

$$(1.81 \times 10^8\ \mathrm{molecules\ of\ HOCl\ lost/(cm^2\ s)})(0.97)(0.5) = 8.78 \times 10^7\ \mathrm{molecules\ of\ Br_2/(cm^2\ s)} \quad (E10)$$

These values are the estimated net gas-phase $Br_2$ production rates from reaction of a steady state mixing ratio of 10 ppt $Cl_2$ or HOCl with sea ice under neutral stability conditions at 248 K. The $Br_2$ formation rate may vary under different meteorological conditions, such as during periods of turbulent atmospheric mixing.

As described in the Introduction, it is not clear which chemical reactions produce the photochemically active bromine compounds that initiate catalytic ozone destruction in the troposphere. Using the rates derived in equations E9 and E10, approximately $3.2 \times 10^{12}$ molecules of $Br_2/cm^2$ of sea ice would be formed in 10 h from reaction of either $Cl_2$ or HOCl. If the $Br_2$ mixes into an air mass 100 m high, then the gas-phase $Br_2$ concentration will be $3.2 \times 10^8$ molecules/$cm^3$, which corresponds to a mixing ratio of approximately 11 ppt. This $Br_2$ mixing ratio is 3.6 times greater than the amount of $Br_2$ formed in the dark reaction of $O_3$ with sea ice as estimated by Oum et al.[22] using similar parameters; this process has recently been suggested as a potential source of active bromine in the Arctic boundary layer.

In conclusion, our results suggest that the $Cl_2$ and HOCl heterogeneous reactions need to be seriously considered alongside other mechanisms that have been proposed to initiate catalytic ozone loss in the troposphere. The amount of $Br_2$ released into the Arctic boundary layer from reactions of $Cl_2$ and HOCl with sea ice may be sufficient to initiate the HOBr autocatalytic bromide oxidation mechanism described in the Introduction. If steady-state $Cl_2$ and HOCl concentrations are high, $Br_2$ produced in the $Cl_2$ and HOCl reactions may even help sustain active bromine levels and catalytic ozone destruction. In addition, this study highlights the connection that exists between the different atmospheric halogen families, emphasizes the need to identify all sources of active chlorine in marine environments, and further illustrates the importance of heterogeneous chemistry that occurs at the surface of ice and aerosol substrates.[39,44]

**Acknowledgment.** This work was funded by a grant from the atmospheric chemistry program at the National Science Foundation. The authors thank Y. Rudich for a helpful discussion and D. Jacob for advice on calculation of the deposition velocity. A.K.H. thanks B. C. Sive for comments on the manuscript.

## References and Notes

(1) Barrie, L. A.; Bottenheim, J. W.; Schnell, R. C.; Crutzen, P. J.; Rasmussen, R. A. *Nature* **1988**, *334*, 138.

(2) Oltmans, S. J.; Schnell, R. C.; Sheridan, P. J.; Peterson, R. E.; Li, S.-M.; Winchester, J. W.; Tans, P. P.; Sturges, W. T.; Kahl, J. D.; Barrie, L. A. *Atmos. Environ*. **1989**, *23* (11), 2431.

(3) Bottenheim, J. W.; Barrie, L. A.; Atlas, E.; Heidt, L. E.; Niki, H.; Rasmussen, R. A.; Shepson, P. B. *J. Geophys. Res*. **1990**, *95* (11), 18, 555.

(4) Wagner, T.; Platt, U. *Nature* **1998**, *395*, 486.

(5) Jobson, B. T.; Niki, H.; Yokouchi, Y.; Bottenheim, J.; Hopper, F.; Leaitch, R. *J. Geophys. Res*. **1994**, *99* (12), 25, 355.

(6) McConnell, J. C.; Henderson, G. S.; Barrie, L. A.; Bottenheim, J.; Niki, H.; Langford, C. H.; Templeton, E. M. J. *Nature* **1992**, *355*, 150.

(7) Fan, S.-M.; Jacob, D. J. *Nature* **1992**, *359*, 522.

(8) Abbatt, J. P. D.; Nowak, J. B. *J. Phys. Chem. A* **1997**, *101*, 2131.

(9) Mozurkewich, M. *J. Geophys. Res*. **1995**, *100* (7), 14, 199.

(10) Sander, R.; Crutzen, P. J. *J. Geophys. Res*. **1996**, *101* (4), 9121.

(11) Tang, T.; McConnell, J. C. *Geophys. Res. Lett*. **1996**, *23* (19), 2633.

(12) Vogt, R.; Crutzen, P. J.; Sander, R. *Nature* **1996**, *383*, 327.

(13) Finlayson-Pitts, B. J.; Livingston, F. E.; Berko, H. N. *Nature* **1990**, *343*, 622.

(14) Impey, G. A.; Shepson, P. B.; Hastie, D. R.; Barrie, L. A.; Anlauf, K. G. *J. Geophys. Res*. **1997**, *102* (13), 16, 005.

(15) Spicer, C. W.; Chapman, E. G.; Finlayson-Pitts, B. J.; Plastridge, R. A.; Hubbe, J. M.; Fast, J. D.; Berkowitz, C. M. *Nature* **1998**, *394*, 353.

(16) Berko, H. N.; McCaslin, P. C.; Finlayson-Pitts, B. J. *J. Phys. Chem*. **1991**, *95*, 6951.

(17) Mochida, M.; Hirokawa, J.; Kajii, Y.; Akimoto, H. *Geophys. Res. Lett*. **1998**, *25*, 3927.

(18) Hanson, D. R.; Ravishankara, A. R. *J. Phys. Chem.* **1992**, *96*, 9441.

(19) Chu, L.; Chu, L. T. *J. Phys. Chem. A* **1999**, *103*, 691.

(20) Kirchner, U.; Benter, Th.; Schindler, R. N. *Ber. Bunsen-Ges. Phys. Chem*. **1997**, *101*, 975.

(21) Fickert, S.; Adams, J. W.; Crowley, J. N. *J. Geophys. Res*. **1999**, *104*, 23, 727.

(22) Oum, K. W.; Lakin, M. J.; Finlayson-Pitts, B. J. *Geophys. Res. Lett*. **1998**, *25*, 3923.

(23) Hirokawa, J.; Onaka, K.; Kajii, Y.; Akimoto, H. *Geophys. Res. Lett*. **1998**, *25*, 2449.

(24) Disselkamp, R. S.; Chapman, E. G.; Barchet, W. R.; Colson, S. D.; Howd, C. D. *Geophys. Res. Lett*. **1999**, *26*, 2183.

(25) See the Discussion section in: Arora, O. P.; Cziczo, D. J.; Morgan, A. M.; Abbatt, J. P. D.; Niedziela, R. F. *Geophys. Res. Lett.* **1999**, *26*, 3621.

(26) Abbatt, J. P. D.; Molina, M. J. *Geophys. Res. Lett*. **1992**, *19* (5), 461.

(27) Benter, Th. Personal communication, University of California, Irvine, 1999.

(28) JANAF Thermochemical Tables, Second Edition, U. S. Department of Commerce NSRDS-NBS37, 1981.

(29) Brown, R. L. *J. Res. Natl. Bur. Stand*. **1978**, *83*, 1.

(30) Hirschfelder, J. O.; Curtiss, C. F.; Bird, R. B. *Molecular Theory of Gases and Liquids*; John Wiley: New York, 1954.

(31) Hanson, D. R.; Ravishankara, A. R. *J. Geophys. Res*. **1991**, *96* (3), 5081.

(32) Hobbs, P. V. *Ice Physics*; Clarendon Press: Oxford, U.K., 1974; section 9.5.

(33) Dankwerts, P. V. *Gas−Liquid Reactions*; McGraw-Hill: New York, 1970.

(34) Steinfeld, J. I.; Francisco, J. S.; Hase, W. L. *Chemical Kinetics and Dynamics*; Prentice Hall: Englewood Cliffs, NJ, 1989.

(35) Finlayson-Pitts, B. J.; Pitts, J. N., Jr. *Chemistry of the Upper and Lower Atmosphere*; Academic Press: San Diego, CA, 2000.

(36) Kumar, K.; Margerum, D. W. *Inorg. Chem*. **1987**, *26*, 2706.

(37) Barrie, L. A. Personal communication, Pacific Northwest National Laboratory, 1999.

(38) Oum, K. W.; Lakin, M. J.; DeHaan, D. O.; Brauers, T.; Finlayson-Pitts, B. J. *Science* **1998**, *279*, 74.

(39) Knipping, E. M.; Lakin, M. J.; Foster, K. L.; Jungwirth, P.; Tobias, D. J.; Gerber, R. B.; Dabdub, D.; Finlayson-Pitts, B. J. *Science* **2000**, *288*, 301.

(40) Barrie, L. A.; den Hartog, G.; Bottenheim, J. W.; Landsberger, S. *J. Atmos. Chem*. **1989**, *9*, 101.

(41) Seinfeld, J. H.; Pandis, S. N. *Atmospheric Chemistry and Physics: From Air Pollution to Climate Change*; John Wiley and Sons: New York, 1998.

(42) The deposition velocity is calculated by[41] $\nu = 1/(R_a + R_b + R_c)$, with resistances $R_a$, $R_b$, and $R_c$ defined as follows. $R_a$ is the resistance due to aerodynamic transport of the gas-phase reactant through the atmospheric surface layer and is expressed by[41] $R_a = (1/u\kappa^2)[\ln(z/z_0)]^2$ for a neutral atmosphere, where $u$ is the wind speed = 10 m $s^{-1}$, $\kappa$ is a dimensionless proportionality factor = 0.4, $z$ is the height of the atmospheric surface layer = 100 m, and $z_0$ is the roughness length = $10^{-5}$ m for ice. In the deposition velocity calculation, the aerodynamic resistance is the overall rate-limiting factor. The true atmospheric mixing may vary in the Arctic troposphere depending on factors such as local wind speed and ice surface roughness. $R_b$ is the resistance due to molecular diffusion of the gas-phase reactant to the ice surface and is expressed by[43] $R_b = z_0/D$, where $z_0$ is the roughness length = $10^{-5}$ m for ice, and $D$ is the molecular diffusion coefficient = 0.147 $cm^2$ $s^{-1}$ for $Cl_2$ in air and 0.105 $cm^2$ $s^{-1}$ for HOCl in air. $R_c$ is the resistance to reactive loss of the gas-phase reactant at the ice surface and is expressed by[35] $R_c = 4/\gamma c$, where $\gamma$ is the reaction probability on a chloride/bromide-ice film at 248 $K$ = 0.0048 for $Cl_2$ and 0.013 for HOCl, and $c$ is the mean molecular speed = 27 100 cm $s^{-1}$ for $Cl_2$ and 31 515 cm $s^{-1}$ for HOCl.

(43) Atkins, P. W. *Physical Chemistry*; W. H. Freeman and Co.: New York, 1990.

(44) Ghosal, S.; Shbeeb, A.; Hemminger, J. C. *Geophys. Res. Lett.*, in press.